

**IMPLICATIONS OF BIMODAL OLIVINE COMPOSITIONS IN VHK BASALTS.** A. J. Gawronska<sup>1</sup>, K. Cronberger<sup>1</sup>, C. R. Neal<sup>1</sup>, <sup>1</sup>Dept. of Civil & Env. Eng. and Earth Sciences, University of Notre Dame, Notre Dame, Indiana, 46556 USA. [agawrons@nd.edu](mailto:agawrons@nd.edu), [kcronber@nd.edu](mailto:kcronber@nd.edu), [neal.1@nd.edu](mailto:neal.1@nd.edu).

**Introduction:** Very high potassium (VHK) basalts are defined as having uncharacteristically high bulk concentrations of K ( $\geq 0.5$  wt.% K<sub>2</sub>O), Rb ( $\geq 10$  ppm), and Ba ( $\geq 100$  ppm), with K/La  $> 500$  [1,2]. They are hypothesized to be derived from high-Al (HA) basalts [1-3], although their petrogenetic pathway remains a mystery. Three hypotheses have been proposed to explain VHK evolution: granite assimilation by HA magmas [1], combined KREEP and granite assimilation by HA magmas [2,3], or impact melt infiltration into HA basalt breccia clasts [4]. As HA basalts are divisible into three distinct groups [5], a wide range of final VHK compositions is possible [1-3].

One notable feature of VHK basalts is the existence of both Fayalitic and Forsteritic olivine crystals within most samples (e.g. [1,2,6]). Despite different possible cooling pathways [2], there appears to be a correlation between the appearance of K-enriched melt and the stabilization of Fayalitic olivine and iron metal (e.g., [1]). This could be due to low silica activities from the incoming alkali melt [1] and could signify changing conditions in the lunar magma in these localities. The goal of this study was to investigate the magma conditions that stabilized Fayalitic olivine in VHK basalts.

*14181,8:* This basalt is approximately 1 cm<sup>3</sup> and weighed 2.48g when collected as a rake sample [6]. Thin section 8, used in this study, is composed of two pieces – the larger called “A” and the smaller “B” (Fig. 1). There are not enough plagioclase crystals in these clasts to construct a crystal size distribution (CSD) analysis ( $<250$  crystals [8]). *14305,388:* Sample 14305 is a 2497g breccia [6]; thin section 388 is composed of a basalt clast with an adhering breccia matrix. CSD analyses have revealed that 14305,388 plots close to the impact melt field defined by [9].

**Methods:** Photomicrographs were gathered using a Nikon petrographic microscope in reflected, non-polarized, and cross polarized light. The samples were then analyzed using a CAMECA SX-50 electron microprobe (EMP) to gather mineral data and produce element maps compiled through *ImageJ* (Figs. 1&2). The largest crystals were further analyzed for trace elements using LA-ICP-MS via a New Wave Research UP213 laser and a Thermo Finnigan Element 2 high resolution inductively coupled plasma mass spectrometer. 3 Mg- and 3 Fe-olivines were chosen for analysis in each sample, following methods outlined by [10].

**Results and Discussion:** *EMP:* Element data gathered revealed that both samples have relatively primi-

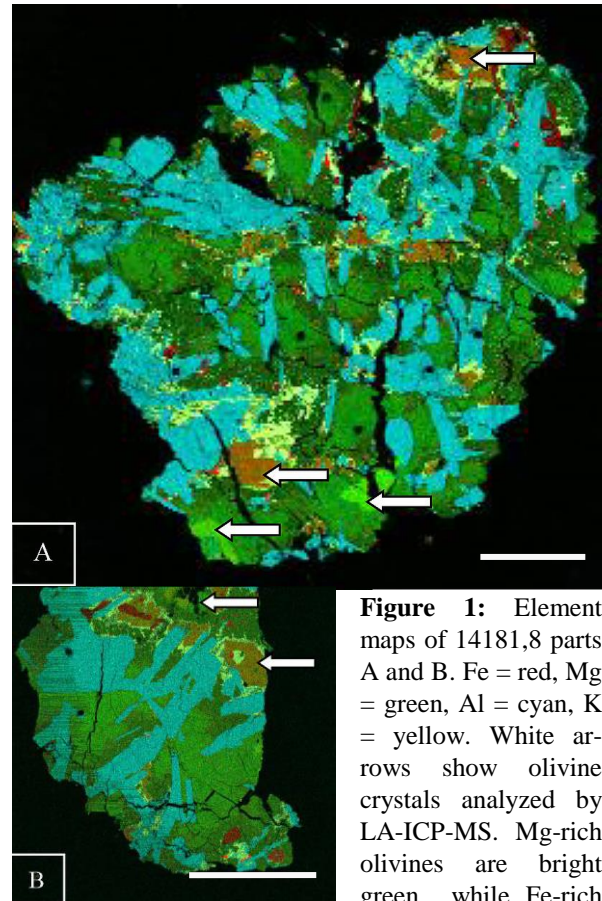


**Figure 1:** Element maps of 14181,8 parts A and B. Fe = red, Mg = green, Al = cyan, K = yellow. White arrows show olivine crystals analyzed by LA-ICP-MS. Mg-rich olivines are bright green while Fe-rich are orange. Yellow K-feldspar generally surrounds the Fe-olivines as well as nodules of Fe-metal, but does not touch the Mg-olivines. Scale bar represents 0.5 mm.

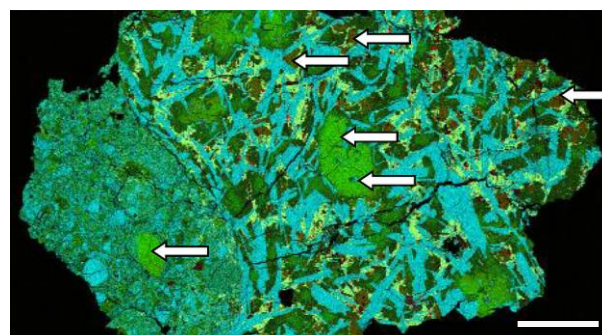


**Figure 2:** 14305,388 element map – Fe = red, Mg = green, Al = cyan, K = yellow. White arrows again denote analyzed olivine crystals – Fe-olivines are orange-brown and small, while Mg ones are larger. Yellow K-feldspar again surrounds Fe-olivines and red Fe-metal. Scale bar represents 1 mm.

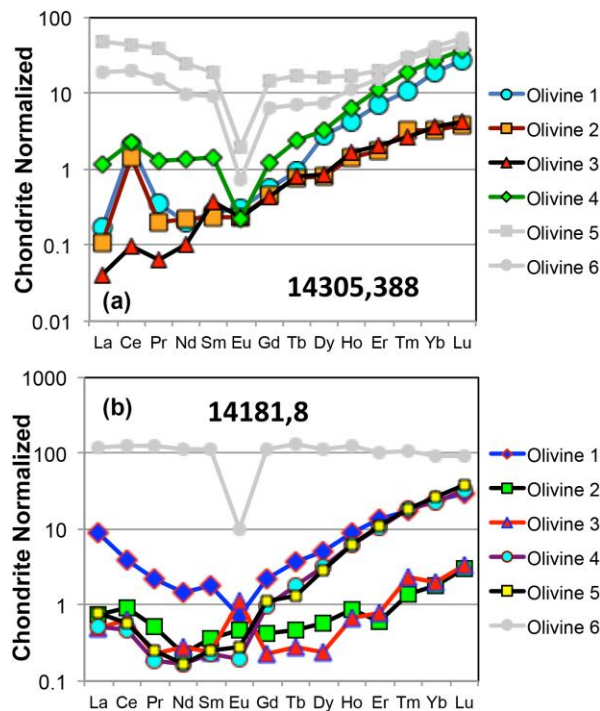


**Figure 3:** Olivine rare earth element profiles. 14305,388 olivine 5 and 6 and 14181,8 olivine 6 are gray to indicate contamination.

tive Mg-olivines that are chemically distinct from Fe-olivines ( $Fo_{MgOlivine} > 60$ ,  $Fo_{FeOlivine} < 40$ ) as seen previously [1,7]. Interstitial spaces appear to be dominated by infiltrating K-rich melt that crystallized K-feldspar without the breakage of surrounding crystals – Fe-olivines are found in this K-rich matrix (Figs. 1&2). The olivine crystals in 14181,8 do not appear to be significantly different in size despite different compositions (Fig. 1) so the cooling regime does not appear to change with infiltration of new material. 14305,388, however, has two large Mg-olivine crystals which suggest slow initial cooling. There are also many relatively small Fe-olivines, which implies that once K-rich melt infiltrated the sample must have cooled quicker than previously. This could reflect the assimilation process as energy would be removed from the melt to melt granite material, resulting in smaller Fe-olivines. The smaller Fe-olivines could also be a product of impact melt infiltration, as the reaction between a melt and a solid would also produce small olivines.

**LA-ICP-MS:** Trace element data calculations revealed that olivine 6 from 14181,8 and olivines 5 and 6 from 14305,388 were contaminated by a Ca phosphate phase, resulting in highly enriched REE profiles (Fig. 3) and uncharacteristically high Th. Therefore, these points are not included in subsequent plots. Olivines 2 and 3 in both samples are Mg-rich and are visibly less enriched in heavy REEs than the other, Fe-rich oli-

vines. It is important to note that 14305,388 olivine 1 is an Mg-olivine in breccia matrix, and its heavy REE content is similar to that of Fayalitic olivines, although it is selectively contaminated in the light REEs; that could be due to impact melt influence [4,10]. In both samples, higher incompatible element content (i.e. Sc, Ti) is present in Fe-olivines and higher compatible element content (i.e. Co, V, Cr) in Mg-olivines (Fig. 4).

The compositions of these two groups do not overlap, which suggests original HA basalts cooled so that relatively primitive Mg-olivines were insulated from the effects of infiltrating melt. During upward movement through the crust, the incoming K-rich melt pushed the system back to crystallizing olivine.

**Interpretation:** Introduction of alkali material led to stabilization of Fayalitic olivine through a fractionation sequence, supporting [1]. This material, however, appears to be highly fractionated rather than a bulk granite inclusion, consistent with [7]. More work remains to see if olivine compositions can be used to distinguish assimilation vs. impact melt infiltration [4].

**References:** [1] Shervais J.W. et al. (1985) PLPSC 16 in JGR 90, D3-D18. [2] Neal C. R. et al. (1988) PLPSC 18, 121-1 37. [3] Neal C.R. et al. (1988) PLPSC 19, 147-161. [4] Roberts S. E. and Neal C.R. (2018) GCA accepted. [5] Neal C. R. and Kramer G. Y. (2006) Am. Miner. 91, 1521-1535. [6] Lunar sample compendium, 14181, 14305 <https://www-curator.jsc.nasa.gov/lunar/lsc/index.cfm>. [7] Cronberger, K. et al. (2016) LPS XLVII, Abstract #1211. [8] Morgan D.J. & Jerram D.A. (2006) JVGR 154, 1-7. [9] Neal C.R. et al. (2015) GCA 148, 62-80. [10] Fagan A. L. et al. (2013) GCA 106, 429-445.

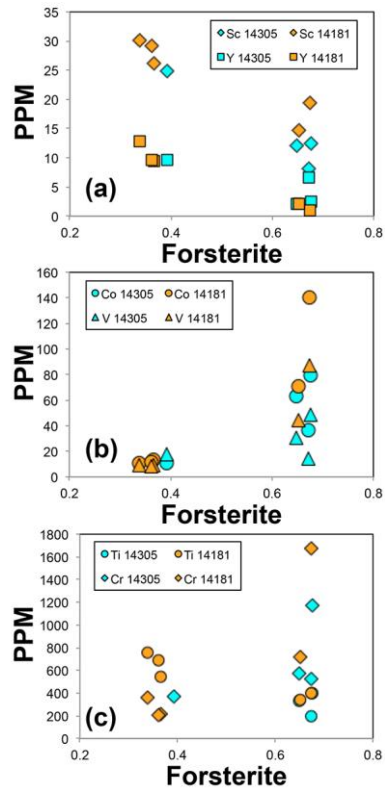


**Figure 4:** Compiled trace element data as compared to Fo content.